Galaxy population properties in the rich clusters MS0839.8+2938, 1224.7+2007 and 1231.3+1542[1]

J.B. Hutchings, L. Edwards
Dominion Astrophysical Observatory
Herzberg Institute of Astrophysics, National Research Council of Canada
5071 W. Saanich Rd., Victoria, B.C. V8X 4M6, Canada

ABSTRACT

This paper discusses the galaxy populations of three rich clusters, with redshift 0.19 (0839+29), 0.24 (1231+15), and 0.32 (1224+20), from the database of the CNOC1 consortium. The data consist of spectra of 52 cluster members for 0839+29, 30 members for 1224+15, and 82 members for 1231+15, and there are comparable numbers of field galaxy spectra. 0839+29 is compact with no strong radial gradients, and possibly dusty. 1224+20 is isolated in redshift, has low velocity dispersion around the cD galaxy, and low 4000Å break. 1231+15 is asymmetrical and we discuss the possibility that it may be a recent merger of two old clusters. We find few galaxies in 0839+29 and 1231+15 with ongoing or recently truncated star-formation.

Subject headings: galaxies: clusters: individual (0839+29, 1224+20, 1231+15), galaxies: evolution, galaxies: stellar content

1. Introduction and data

This paper continues the discussions of galaxy populations of rich clusters of intermediate redshift, based on the CNOC1 project database. The project and basic data have been described by Yee, Ellingson and Carlberg (1996), and similar cluster investigations have been published by Abraham et al (1996) and Morris et al (1998) for the clusters A2390 (z=0.23) and MS1621.5+2640 (z=0.42) (papers 1 and 2). Further discussion of the whole cluster ensemble has been carried out by Balogh et al (1999). We

[1]Based on observations with the Canada France Hawaii Telescope, which is operated by the NRC of Canada, CNRS of France, and the University of Hawaii

also discuss VLA radio imaging data for the clusters 0839+29 and 1224+20, which were obtained in conjunction with the CNOC1 program. The VLA data were obtained with the C configuration at wavelengths 20cm and 6cm. Some details of the VLA observations are given in paper 1.

The clusters selected for this paper were chosen from the CNOC database because of their sample size, redshift comparison with those of papers 1 and 2, and the radio imaging data. The investigation follows the same lines as papers 1 and 2: discussion of the spatial distribution of spectral properties and colours, particularly with projected distance from the central galaxy, and fitting of models that indicate the stellar content and star-formation history of galaxies in the cluster. We also compare the properties of different clusters.

The data are described by Yee, Ellingson, and Carlberg (1996), and papers 1 and 2 contain full intoductory material on the galaxy population studies: the reader is referred to those publications for details. Our treatment of the data is the same as in papers 1 and 2. As in paper 2, we have used the GISSEL96 models for comparison with the measurements from the data. Table 1 summarizes the data and properties of the three clusters.

The D4000 index is measured the same way as in the other cluster papers (Hamilton 1995). Balogh et al (1999) use a narrower definition in their measure which may be less prone to systematic effects of redshift, passband, and reddening. We have compared measures made with the 'standard' passbands and two reduced passbands of Balogh (private communication). For the clusters in this paper, the mean ratio of narrow to standard passband measures ranges from 1.00 to 1.06 for an intermediate bandpass, and from 0.85 to 0.90 for a very narrow one. We do not think this indicates any significant systematic effect in retaining the original Hamilton passbands, and this has the advantages of enabling direct comparison with the two other CNOC cluster papers. As in the other papers, the same measures are made in the model spectra as the observed.

We did look for systematic differences with Balogh et al's results by counting galaxies in the boxes they define in the D4000/Hδ plane. Balogh et al count galaxies in these boxes in order to compare their results with those of Barger et al (1996). The boundaries chosen pass through the centre of the dense distribution of galaxies, so that the numbers are very sensitive to the exact placement of the boundaries. Using the Hamilton D4000 measure, we can closely match the counts of Balogh et al with the D4000 boundary moved from 1.45 to $\sim$1.65, which is also close to the variation introduced by bandpass choice, as noted above. In view of the sensitivity of number counts to the chosen boundaries, and the relatively small numbers of galaxies in our clusters, we do not think such number counts are particularly useful for this paper. With the above D4000 normalisation, they are however, the same as those of Balogh et al for the whole CNOC cluster sample, within the poisson

scatter expected for the number counts in the individual clusters in this paper.

The Hδ measures have also been the subject of discussion. Abraham et al (1996) used a combination of two different measures intended to account for the changing contamination of the continuum bands with different stellar populations. Morris et al (1998) noted that since the same measures are made on model and observed spectra, and the conclusions are unaffected, only one of the Hδ measures was used. However, a correction of 1.7A was applied to account for the different resolution of the model and observed spectra. Most recently, Balogh et al have claimed that the sampling has little effect on the Hδ measure, and omitted this correction. Rather than add to this debate, in this paper, we have followed Morris et al to enable direct comparison with their results.

Balogh et al (1999) have found that the formal uncertainties in some line indices underestimate the reproducibility of their measurements. For comparison with the cluster papers 1 and 2, we have not applied any correction factors to the errors we display. The mean scale factors to these error bars derived by Balogh are 2.0, 1.4, and 1.4 for D4000, Hδ, and [O II], respectively.

For each cluster we discuss membership and define a sample of field galaxies from the same sample. There are a few galaxies which lie at the edge of the clusters which may not (yet) be bound members, and these are designated near-field galaxies, as in paper 2. We use the same definition of these as Balogh et al, although they stand out clearly to the eye in the redshift-radius plots. Galaxy colours from the direct images and spectral indices (D4000, Hδ, and [O II]) from the spectra are plotted with clustocentric distance. The galaxies are grouped in radius bins and the measured quantities of each subset compared with the same measures on stellar population models for galaxies. We present mean properties of various subsets of the galaxies, and present mean spectra for several of these subsets. We also show the spatial distribution of some subsets of the galaxy populations.

We discuss the inferred stellar populations and galaxy evolution for the clusters and compare the results for all the CNOC clusters thus analysed.

2. 0839+29

This cluster (along with 1224+20) has been discussed as a cooling flow cluster on the basis of extended Hα emission, by Donahue, Stocke, and Gioia (1992), and from X-ray imaging by Nesci, Perola, and Wolter (1995).

The membership of the cluster from the sample spectra is illustrated in figure 1.

Figure 2 shows the colour gradient with magnitude and radius, and from this we adopt the red sequence of members at g-R>0.75. The blue and red galaxies fall within the same cusp envelope in Figure 1 (which seem to be poorly sampled at radii above ∼400"), so the colour cut is not particularly significant. We have labelled 3 galaxies that lie outside a symmetrical cusp envelope but very close to the cluster, as 'near-field'. These are all blue, as was found for similar galaxies in 1621+26.

The cluster is relatively compact within the large size of fields sampled (see Table 1). Only two galaxies with the cluster redshift are seen further than 463" from the central galaxy, compared with 1400" for the similar redshift A2390, and 700" for the higher redshift 1621+264 in papers 1 and 2. Carlberg, Yee, and Ellingson (1997) compare the dynamical parameters of the CNOC clusters, and 0839+29 has the lowest virial radius of all, except for the binary cluster 0906+11.

The spatial distributions of some subsets of the galaxies are shown in Figure 3. The field galaxies used for comparison lie in the redshift range 0.17 to 0.22. There are 25 of these and their redshift range is small enough that no colour corrections are needed for model comparisions. In any case, in this paper we do not show any color models.

As in papers 1 and 2, we choose the colour, D4000, Hδ, and [O II] spectral measures for discussion and modelling for stellar populations. Figure 4 shows these plotted with (log) radius, and compared with the non-member sample. The measurements and error estimates were made using the same algorithm as in papers 1 and 2. Table 2 shows mean properties of various subsets of the galaxies. This table also includes indices of other lines that are sensitive to stellar population. The table also includes mean values for extreme [O II] and Hδ as defined. Such quantities are shown for all three clusters as different ways of summarizing the data.

There is a group of 15 galaxies with redshift near 0.217 that appear to be clustered. They are located close to each other in the sky, centred about 100" from the centre of 0839+29. Table 2 also shows their properties: they seem to have active star-formation and a young stellar population. There is a group of 4 galaxies that lie at an intermediate redshift between the main and this small cluster, that has even younger populations. These appear as a group in the sky, but some 200" to the other side of the main cluster centre. Thus, they are not obviously involved with either cluster, but may be a small group on their own.

In Figure 4 we have plotted measurements with log radius: the cD galaxy is arbitrarily placed at 0.41, since it lies at zero radius. The plot shows an apparent gradient of D4000 with radius in the cluster, particularly beyond 250". In all the data the [O II] emission line

is not seen below redshift ∼0.2 because of the spectral bandpass, but other field samples and those above z∼0.2 show no trend across the cluster redshifts that might concern our camparison with cluster members. The suggested smaller cluster at z=0.217 does stand out in [O II] behaviour. The colour plot shows little change in the red sequence, and there are a few Hδ strong galaxies seen in the central part of the cluster. The majority of the cluster population seems to have evolved passively for some time, and there is little accretion happening. The three near-field galaxies do stand out as younger and forming stars. One of them has an Seyfert spectrum, whose Hδ emission is off-scale in the plot. We note that the spectral passband prevents [O II] measures in the lower redshift field galaxies.

Figure 5 shows mean spectra of the major subgroups. These are derived from the galaxies with best signal in each group, but we have checked that their mean measured properties are still representative of the whole subgroup. These may be compared with similar mean spectra from papers 1 and 2, and the other clusters in this paper, but have no remarkable properties in that context.

We have divided the members into three radial distance groups of roughly equal population, and with boundaries close to radii where measured quantities change. Figure 6 shows plots of measured quantities for these subsets, and also the field sample. The diagrams also show models computed from GISSEL96, as in paper 2. The upper curve is for a 1 Gyr starburst followed by passive evolution, and the lower curve is for exponentially decreasing star-formation with a timescale of 4 Gyr. Both models are for solar abundance, and the Hδ index is corrected for spectral resolution as in paper 2. Paper 2 also discusses in more detail the effects of different abundances and initial mass funtion.

These plots show there are several blue galaxies with fairly strong Hδ in the central region (or projected on to it, as their high velocity dispersion suggests). This is unusual in the central parts of these rich clusters. There are also a few galaxies with ongoing star-formation in the outer regions. As noted from the other plots above, there is an old population seen at all radii among the members.

In Figure 19 and Figure 20 we show the variation of D4000 and Hδ with age together with the histograms of these quantities in all three clusters. At the redshift of 0839+29 we expect the oldest populations to be some 12 Gyr. The bulk of the cluster population seems to be signficantly younger than this, and from figure 6 we see little radial gradient. The outer cluster has no old populations. The field galaxy population is similar to the outer cluster members. The inner cluster has several galaxies with higher Hδ index than the field or the models, as seen in 1621+26. This may result from a truncated IMF in the inner cluster galaxy populations, as noted in paper 2.

We find 4 galaxy coincidences with radio sources in the VLA images. These are summarized in Table 3. The cD galaxy is the strongest source. The second radio source is the Seyfert galaxy. It is a disk galaxy with a bright nucleus. The next source is a red galaxy within the central cluster, with a fairly young stellar population. It is asymmetrical and possibly interacting. The fourth galaxy has no spectrum but is clearly interacting and is probably a foreground galaxy, judging by its size and brightness. Table 3 summarizes the radio source identifications.

In order to investigate the galaxy environments of cluster members, we created a table of the distance and magnitude of galaxies within 100 pixels (∼33 arcsec) of each, from the imaging catalogue of the field, which extends to magnitude 24 and fainter. Plots from these numbers do not reveal any connection between spectra and apparent small groups. The most clustered members do not have unusual spectral measures or active star-formation.

3. 1224+20

The data for this cluster are published by Abraham et al (1998). This cluster has been discussed as an example of velocity bias by Carlberg (1994), and Fahlman et al (1994) also find a weak lensing mass that exceeds the virial mass by a factor of more than 2. Lewis et al (1999) report an X-ray mass estimate which is consistent with the dynamical one. Carlberg, Yee and Ellingson (1997) show from the CNOC database that the cluster radius is lower than average for the group, and the velocity dispersion close to average at 798 km s^{-1}. In addition to the CNOC database, we also have VLA maps at 20cm and 6cm of the cluster.

The CNOC spectroscopic database is relatively small for this cluster, with 75 spectra, of which 30 are considered members. Among the sample, there is a very clear redshift separation of members and field galaxies, but the sample does not indicate the usual central velocity spread among the members. The colour plots in Figure 7 suggest the red sequence colour cut-off at g-R=0.95: however, with this cut, the blue member galaxies do not show the usual larger scatter in redshift-radius distribution than the red members (see Figure 8). It may be the lack of central velocity spread among the CNOC members that causes the virial mass discrepancies noted above. The densest grouping of cluster members occurs some 80 arcsec away from the cD galaxy nominally regarded as the cluster centre. This dense group does not have a special redshift, and the low velocity outliers do not form a spatial group, so there is no obvious simple substructure. Figure 9 shows the distribution of galaxy subsets in the sky.

The radial gradients and field comparisons of measured quantities are shown in Figure 10. The cluster members generally have considerably more evolved stellar populations than the field. Some of the blue members do have younger populations, but do not show much star-formation. The values of D4000 however, are unusually low for an evolved population, with an average for red members of 1.7, compared with values well over 2 for other CNOC clusters (see figure 19). The measures were made with the same code as all other spectra, and are small with any definition of D4000 index and redshift, so this suggests that the cluster may have formed fairly recently, and that star-formation turned off not very long ago.

The mean spectra of representative subsets are shown in Figure 11. The low D4000 break is also seen here. Table 4 gives the mean measured values. We looked at the off-centre compact group ('A') separately, but they do not show any interesting difference that suggests they are a subgroup, as also noted above.

Figure 12 shows model measures and the data in two radial bins, and the field. There is little radial gradient in D4000 which is also consistent with recent cluster-wide evolution in this quantity shortly after star-formation ceases. The field galaxies in this region have very blue colours, presumably indicating young stellar populations. The member and field galaxy colours are consistent with this suggestion. There is little or no colour gradient in the red sequence within the cluster.

In view of the virial peculiarities noted for the cluster, the low velocity dispersion about the cD galaxy, and the dense grouping of members off the centre, we investigated the consequences of adopting this dense region as cluster centre. The redshift/radius relationship does look more normal: it is highest at this centre, although still low. This centre also shifts the two low D4000 (young population) galaxies out of the central 100" radius bin, which is also more normal. The second brightest member galaxy in our sample (18.6 compared with 18.0 for the cD) lies near this new centre, at +91, -47 in arcsec from the cD. However, its redshift is far from the cluster mean at 0.3198, and it has an old population and red colour. The dymanic situation of this cluster needs more detailed investigation.

Among the radio sources in the field, only four correspond with galaxies in the image. The brightest two sources (15 - 20 mJy at 20 cm) are large foreground galaxies for which we have no spectrum, or hence redshift. The next source has flux 2.6 mJy at 20 cm, and is a 16mag foreground galaxy at redshift 0.05. The last source identified has 20cm flux 0.4 mJy, and is measured at 3.8" from the cD galaxy, which we adopt as the identification. Thus, there is only one weak cluster source which is the cD.

Searching the photometric catalogue for faint companions, we find the crowded region at radius 65" - 85" also stands out down to 24th magnitude. In addition, there are few faint galaxies inside this radius. This suggests that the region around the cD galaxy (if it is the cluster central region) has been cleared of faint galaxies or has enough extinction to hide background galaxies.

4. 1231+15

This cluster has a larger radius and lower velocity dispersion than the other two. The sample includes three masks in the central field, and one each to the north and south, so that the central region is well sampled. The red sequence cutoff is easily defined at g-R=0.7, as there is a wide gap with no galaxies of colours between 0.62 and 0.76 (Figure 13). The red sequence colour is normal for its redshift among CNOC clusters, and has a clear gradient with radius and magnitude. The redshift-radius plot (Figure 14) shows a well virialised distribution of galaxies, both red and blue, with 3 near-field galaxies (in the radius range 250-300 arcsec) which are red. These do not form a close physical group, in spite of the very similar redshifts. The cD galaxy has a velocity some 250 km s^{-1} lower than the cluster mean. The galaxy distribution on the sky is asymmetrical about the cD (Figure 15), suggesting that possibly the cluster has merged from two. We investigated this by splitting the galaxies into groups, as shown in the diagram. The redshift-radius plots are very similar for the two, but group 1 has younger population indicators. Table 4 shows differences in this sense in all mean indices, each at about 1σ level.

The plots of measured properties with (log) radius are in Figure 16. The cluster is characterised by high values of D4000 (along with other line measures indicating old or high abundance populations). This indicator is higher for group 1 than group 2. The radial gradient of spectral features seen in Figure 15 is unusual in showing undulations, and this too may be explained by a different population (and hence history) of galaxies in the two main groups. Figure 17 shows mean spectra of representative subsets.

Figure 18, 19, and 20 show the comparison with models. This cluster has a significant number of high Hδ red galaxies, and high D4000 values, particularly in the mid-range of radius. This could arise from a higher abundance in the stellar populations, possibly by being formed from galaxies that had long periods of star formation before forming the cluster. There are similar galaxies in the field, as well as some (still the majority) that have ongoing star-formation.

Looking for faint companions to cluster galaxies, we find that many of the 82 have

several galaxies within 5 arcsec, and 13 of them look like compact groups in the sky. Most of those are unremarkable red galaxies but there are three with blue colours and/or active star-formation. Of those, the bluest is in a populous group of 10, while the other two are have 3-4 very close companions. In these cases at least it seems possible that the stellar populations are affected by local interactions within the groups. This cluster has a higher density of faint galaxies than the other two. The average number of galaxies to the catalogue limits are 45 for 1231+15, 20 for 1224+20, and 15 for 0839+29. Comparing the magnitude distributions, the 0839+29 catalogue is less complete to 24 mag, while the 1231+15 is the most complete. The distributions of slit masks across the three clusters are similar (Table 1), but less centrally concentrated in 0839+29. However, the groups of around the star-forming member galaxies in 1231+15 are not at the faint limit and would be visible in either of the other two catalogues.

5. Comparison and discussion

We have presented the same plots and model comparisions for the three clusters. We have not done this in the same detail as in papers 1 and 2, focussing principally on Hδ and D4000 in the model discussions. Other quantities are shown in the data plots and tables.

The colours of the red sequences for the clusters and those of papers 1 and 2 (A2390 and 1621+26) follow a progression with redshift, except for 0839+29 which is redder by some 0.15 in g-R. This may indicate the presence of some dust in this cluster, since the line indices do not correspond with high abundance or age. This cluster may contain populations of different ages or abundance, as the D4000 distribution appears bimodal (see figure 19). This is seen in 1621+26, but in 1621 the main population is old/high abundance while in 0839+29 it is young/low abundance.

The cluster 1224+20 has remarkably low D4000, suggesting that its stellar population is either of low abundance or that the cluster itself has only formed, and hence stopped star-formation, recently. As noted, the discussions of velocity suggest that the cluster may be in an early stage of its dynamical evolution too. The highest concentration of member galaxies and the largest velocity spread is found some distance from the cD galaxy. The lack of star-forming members and strong Balmer absorbers also suggest that there is little current infall, since infall is regarded as truncating or restarting star-formation. The lack of neighbouring redshifts among the field sample also is consistent with this scenario.

The cluster 1231+15 has a wide spread of age/abundance, and a complex gradient of D4000 with radius. As we have discussed, there are suggestions of a recent merging of

major subclusters to form this cluster. The relatively high fraction of star-forming and Hδ strong galaxies in this cluster may also result from this.

We are grateful to David Schade and Simon Morris for help with the CNOC database and with the GISSEL models.

References

Abraham R.G. et al 1996, ApJ, 471, 694 (paper 1)

Abraham R.G., Yee H.K.C., Ellingson E., Carlberg R.G., Gravel P., 1998, ApJS, 116, 231

Balogh M.L., Morris S.L., Yee H.K.C., Carlberg R.G., Ellingson E., ApJ (in press: astro-ph 9906470)

Barger A.J. et al, 1998, ApJ, 501, 5223.

Carlberg R.G., Yee H.K.C., and Ellingson E., 1997, ApJ, 478, 462

Carlberg R.G., 1994, ApJ, 434, L51

Donahue M., Stocke J.T., Gioia I.M., 1992, ApJ, 385, 49

Fahlman G., Kaiser N., Squires G., and Woods D., 1994, ApJ, 437, 56

Hamilton D., 1985, ApJ, 297, 371

Lewis A.D., Ellingson E., Morris S.L., Carlberg R.G., 1999, ApJ in press (astro-ph 9901062)

Morris S.L., et al, 1998, ApJ, 507, 84 (paper 2)

Nesci R., Perola G.C., Wolter A., 1995, A&A, 299, 34

Yee H.K.C., Ellingson E., and Carlberg R.G., 1996, ApJS, 102, 289

Captions to Figures

Fig. 1.— Members of cluster 0839+29 in the sample. The nearfield galaxies may not be virialised members but lie far from the nearest field galaxies.

Fig. 2.— Plots of colour with magnitude and clustocentric radius. We adopt a colour cut of 0.75 to define the red sequence of members.

Fig. 3.— Distribution of 0839+39 field galaxies in the sky.

Fig. 4.— Properties of 0839+29 member and field galaxies with projected distance from cluster centre.

Fig. 5.— Representative mean spectra of subgroups in 0839+29 field. Spectra are derived from 6-10 galaxies with good signal and properties close to the subgroup means. They are shifted to the mean cluster redshift and smoothed.

Fig. 6.— Hδ and D4000 indices for 0839+29 members and field galaxies, compared with the same measures from GISSEL96 models. The dashed line shows passive evolution after a 1 Gyr starburst, and the solid line represents exponentially decreasing star-formation with the timescale of 4 Gyr.

Fig. 7.— Plots of colour with magnitude and clustocentric radius for MS1224.7+2007. We adopt a colour cut of 0.95 to define the red sequence of members.

Fig. 8.— Members and nearby galaxies in redshift space around the centre of 1224+20.

Fig. 9.— Distribution of 1224+20 field galaxies in the sky.

Fig. 10.— Properties of 1224+20 member and field galaxies with projected distance from cluster centre.

Fig. 11.— As Figure 5, for cluster 1224+20.

Fig. 12.— As figure 6, for cluster 1224+20. The solid lines are solar abundance models and the dashed line is for 1/5 solar.

Fig. 13.— Plots of colour with magnitude and clustocentric radius for MS1231+1542. We adopt a colour cut of 0.70 to define the red sequence of members.

Fig. 14.— Members and nearby galaxies in redshift space around the centre of 1231+15.

Fig. 15.— Distribution of 1231+15 field galaxies in the sky.

Fig. 16.— Properties of 1231+15 member and field galaxies with projected distance from cluster centre.

Fig. 17.— As Figure 5, for cluster 1231+15.

Fig. 18.— As Figure 6, for cluster 1231+15. Note the large population of cluster galaxies with high Hδ and D4000.

Fig. 19.— Growth of D4000 index from GISSEL96 models. The post-starburst models have passive evolution after a 1 Gyr starburst, and the star-forming models decrease with 4 Gyr timescale. The star-forming models have very little change with abundance. The panels superpose the distribution of D4000 indices for the members of the three clusters studied.

Fig. 20.— As Figure 19, but for Hδ.

Table 1. CNOC data on clusters analysed

Cluster	z	Members	Field	# Fields[a]	Comment
0839+29	0.19	52	99	E,C(2),W1(2),W2(2)	VLA, Cooling flow
1224+20	0.32	30	45	C(2)	VLA, Cooling flow
1231+15	0.24	82	78	C(3),N,S	

[a]location of ∼10' fields in cluster, (with number of slit masks)

Table 2. Mean properties of galaxies in 0839+29

Group[a]	#	g-R	D4000	Hδ	[OII]	R[b]	z	m_R	Hγ	CaK	g band
Red	38	0.89	2.07	2.0	-0.6	132	0.1935±0.0031	19.5	1.2	11.7	6.4
Blue	12	0.42	1.51	5.1	-24	254	0.1933±0.0049	19.9	3.6	2.3	3.0
Hδ >4Å	14	0.70	1.89	7.3	-6	134	0.1942±0.0043	19.8	3.5	9.1	5.3
[OII]<-15Å	8	0.46	1.66	4.8	-38	326	0.1926±0.0048	20.1	2.3	4.3	3.2
Radius<85"	18	0.82	1.99	2.2	-6	48	0.1932±0.0045	19.3	2.5	10.3	5.6
Radius 85-200"	20	0.86	2.04	3.4	2	134	0.1939±0.0028	19.7	1.1	10.7	6.2
Radius>200"	12	0.59	1.69	2.4	-20	378	0.1944±0.0034	20.0	1.8	6.0	4.6
Field	25	0.61	1.66	3.9	-23	(313)	0.17–0.22	19.8	1.0	5.2	3.3
Field	99	0.72	1.66	4.7	-27	(385)	0.05–0.48	20.6	1.5	4.6	3.7
Cluster#2	15	0.63	1.72	4.0	-16	(263)	0.2167±0.0018	19.7	1.2	5.8	3.6

[a]cD and Seyfert galaxies omitted; Blue/Red cut at g-R=0.75
Line measures are in Å

[b]Mean projected radius from cD in arcsec

Table 3. Radio sources in 0839+29 field

#	m_R	" from cD (RA, Dec)	RA(2000)	Dec(2000)	Opt-radio (arcsec)	S(20cm,6cm) (mJy)	Notes
1	17.0	0,0	08:42:55.9	29:27:27	0.4	21.2, 1.9	cD galaxy
2	19.1	-52.3, 58.3	08:42:51.8	29:28:25	1.4	3.7, 0.4	Near-field Seyfert
3	19.5	-26.9, 151.9	08:42:53.9	29:29:57	1.1	1.0, -	Member, interacting?
4	19.5	118, 42	08:43:04.9	29:28:08	3.4	0.8, -	Interacting, foreground?

Table 4. Mean properties of galaxies in 1224+20 field

Group[a]	#	g-R	D4000	Hδ	[OII]	R[b]	z	m_R	Hγ	CaK	g band
Red	23	1.24	1.69	1.1	0.3	142	0.3256±0.0037	20.5	2.0	9.7	6.4
Blue	6	0.63	1.33	4.3	-13	139	0.3251±0.0028	21.0	0.9	5.5	3.4
Hδ >3	10	0.87	1.44	5.3	-8	150	0.3255±0.0032	20.9	1.1	5.1	4.0
[OII]<-5	6	0.90	1.46	4.4	-15	108	0.3268±0.0023	21.1	0.0	3.7	3.1
Group A	6	1.25	1.78	2.0	1	89	0.3238±0.0041	20.5	1.9	8.4	7.2
Radius<100"	11	1.14	1.65	2.2	-2	69	0.3249±0.0034	20.6	3.0	8.9	6.7
Radius>100"	18	1.10	1.60	1.6	-3	186	0.3258±0.0035	20.5	1.0	8.8	5.2
Near field	6	0.95	1.41	3.3	-25	240	0.31–0.36	20.4	-0.6	4.1	3.9
Field	45	0.82	1.32	4.1	-27	–	0.05–0.61	20.6	-0.5	7.5	5.5

[a]Without central cD galaxy; Blue/Red cut at 0.95
Line measures are in Å

[b]Mean projected radius from cD in arcsec

Table 4. Mean properties of galaxies in 1231+15 field

Group[a]	#	g-R	D4000	Hδ	[OII]	R[b]	z	m_R	Hγ	CaK	g band
Red	67	0.89	2.28	2.2	-1	201	0.2351±0.0025	19.8	0.6	11.1	6.7
Blue	15	0.40	1.51	6.4	-26	296	0.2347±0.0026	20.2	0.4	5.9	2.7
Hδ >5	22	0.68	1.92	7.9	-8	197	0.2347±0.0027	20.3	-0.5	10.0	4.5
[OII]<-20	13	0.49	1.55	5.0	-38	331	0.2356±0.0025	20.6	-0.6	9.8	4.2
Radius<80"	17	0.92	2.36	1.9	0	47	0.2355±0.0030	19.5	1.6	9.9	7.2
Radius 80-320"	47	0.79	2.16	3.6	-5	190	0.2349±0.0025	20.0	0.3	10.9	5.8
Radius>320"	18	0.70	1.87	2.5	-12	452	0.2349±0.0018	20.1	0.3	8.4	5.2
Near field	3	0.89	2.91	1.5	12	283	0.2283±0.0007	19.0	-0.4	9.4	4.4
Field	19	0.59	1.77	3.8	-15	365	0.24–0.28	20.2	1.6	4.3	2.6
Group A	6	0.91	2.16	2.3	-2	56	0.2366±0.0040	20.1	0.5	6.6	4.7
Group B	15	0.89	2.44	2.2	2	55	0.2342±0.0024	19.4	1.4	12.9	8.4
Group 1	31	0.73	1.98	3.9	-12	286	0.2355±0.0024	20.1	0.1	10.6	5.2
Group 2	16	0.82	2.28	2.7	-4	224	0.2348±0.0025	19.7	0.1	10.2	7.0

[a]g-R Red/Blue cut at 0.70
line measures in Å

[b]Mean projected radius from cD in arcsec

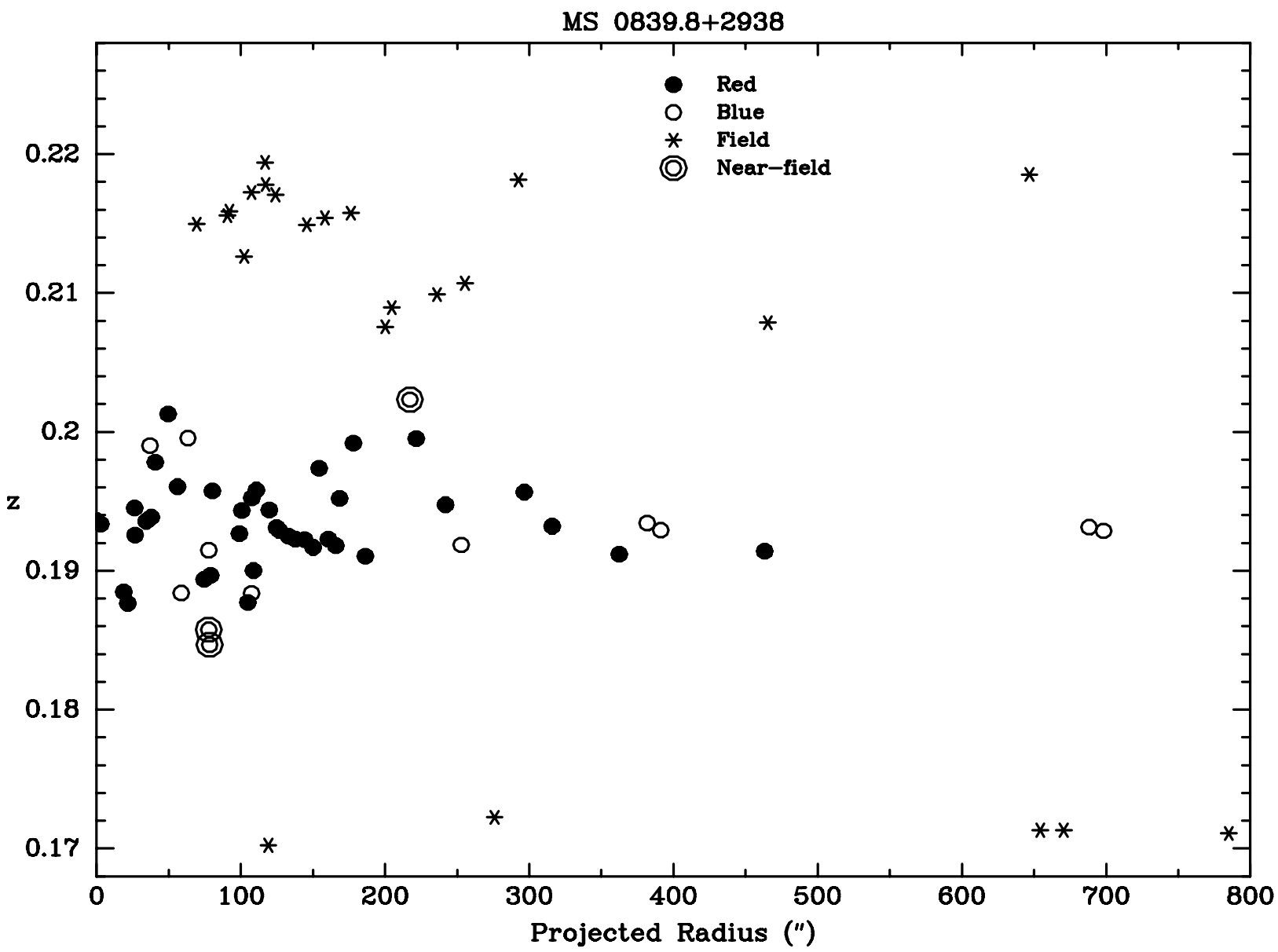
MS 0839.8+2938
Red
Blue
Field
Near−field
z
0.22
0.21
0.2
0.19
0.18
0.17
0
100
200
300
400
500
600
700
800
Projected Radius (")

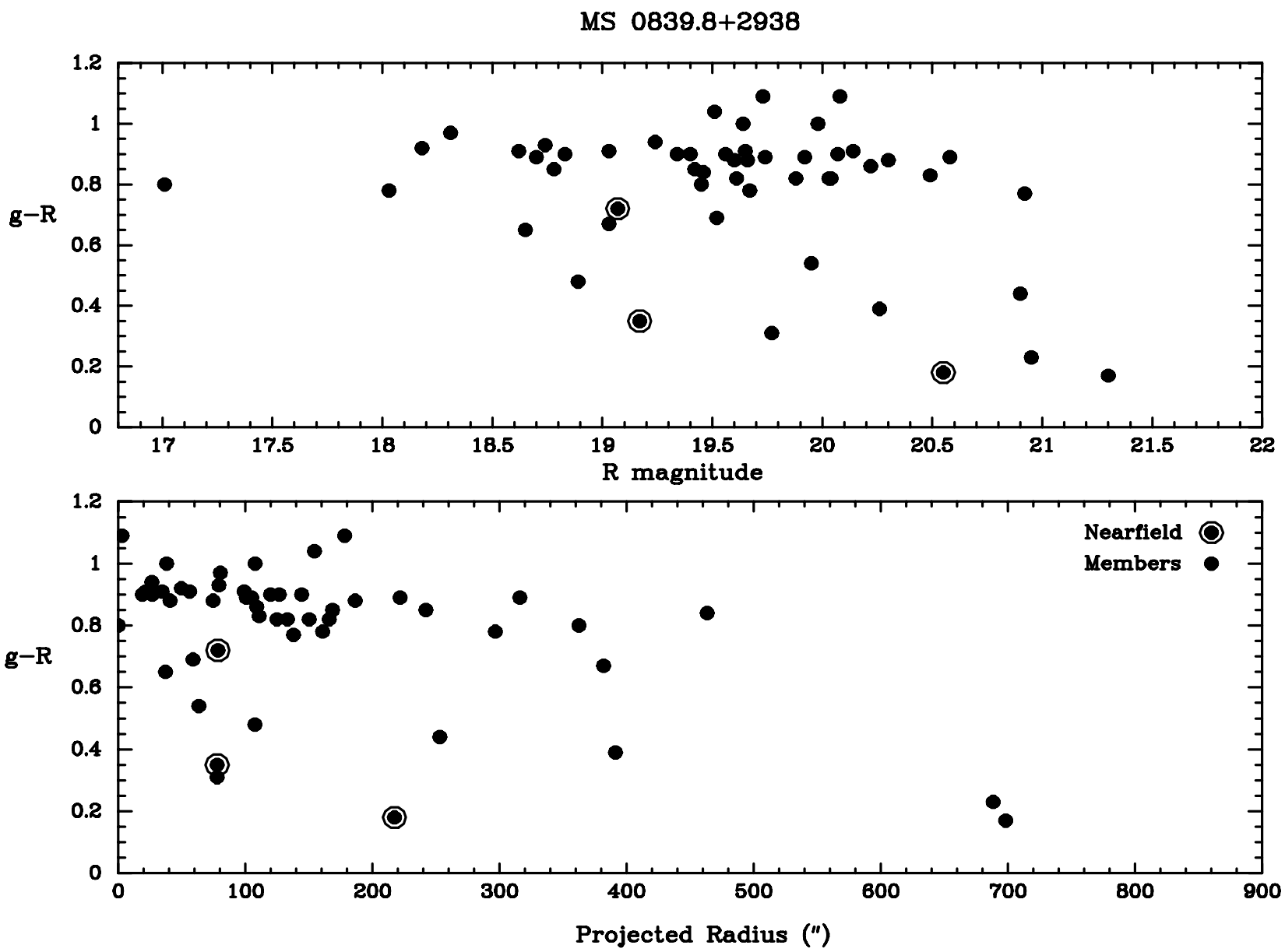
MS 0839.8+2938
g−R
R magnitude
Nearfield
Members
g−R
Projected Radius (")

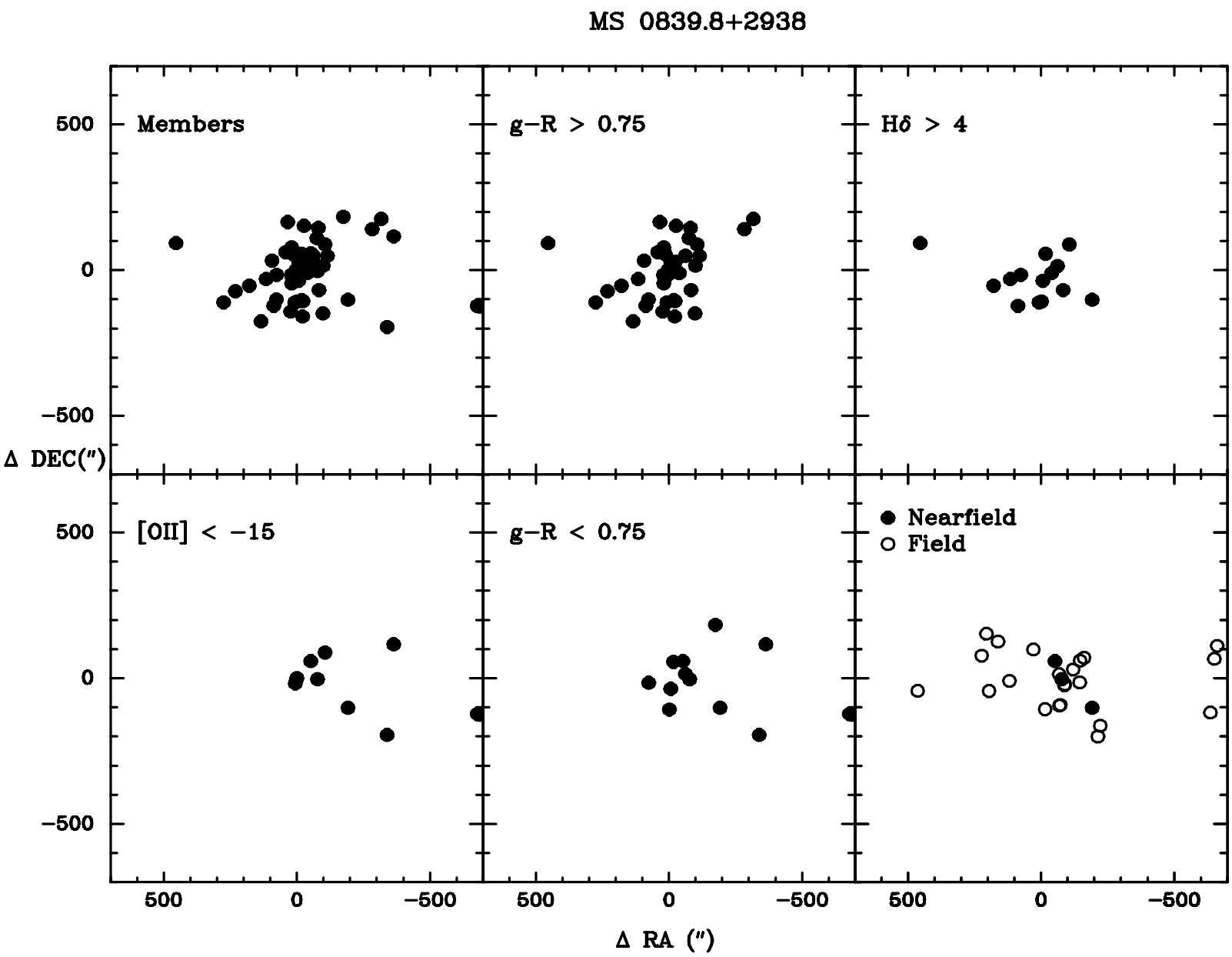
MS 0839.8+2938
Members
g−R > 0.75
Hδ > 4
[OII] < −15
g−R < 0.75
Nearfield
Field
500
0
−500
Δ DEC(")
Δ RA (")

This figure "fig4.gif" is available in "gif" format from:

http://arXiv.org/ps/astro-ph/9912148v1

This figure "fig5.gif" is available in "gif" format from:

http://arXiv.org/ps/astro-ph/9912148v1

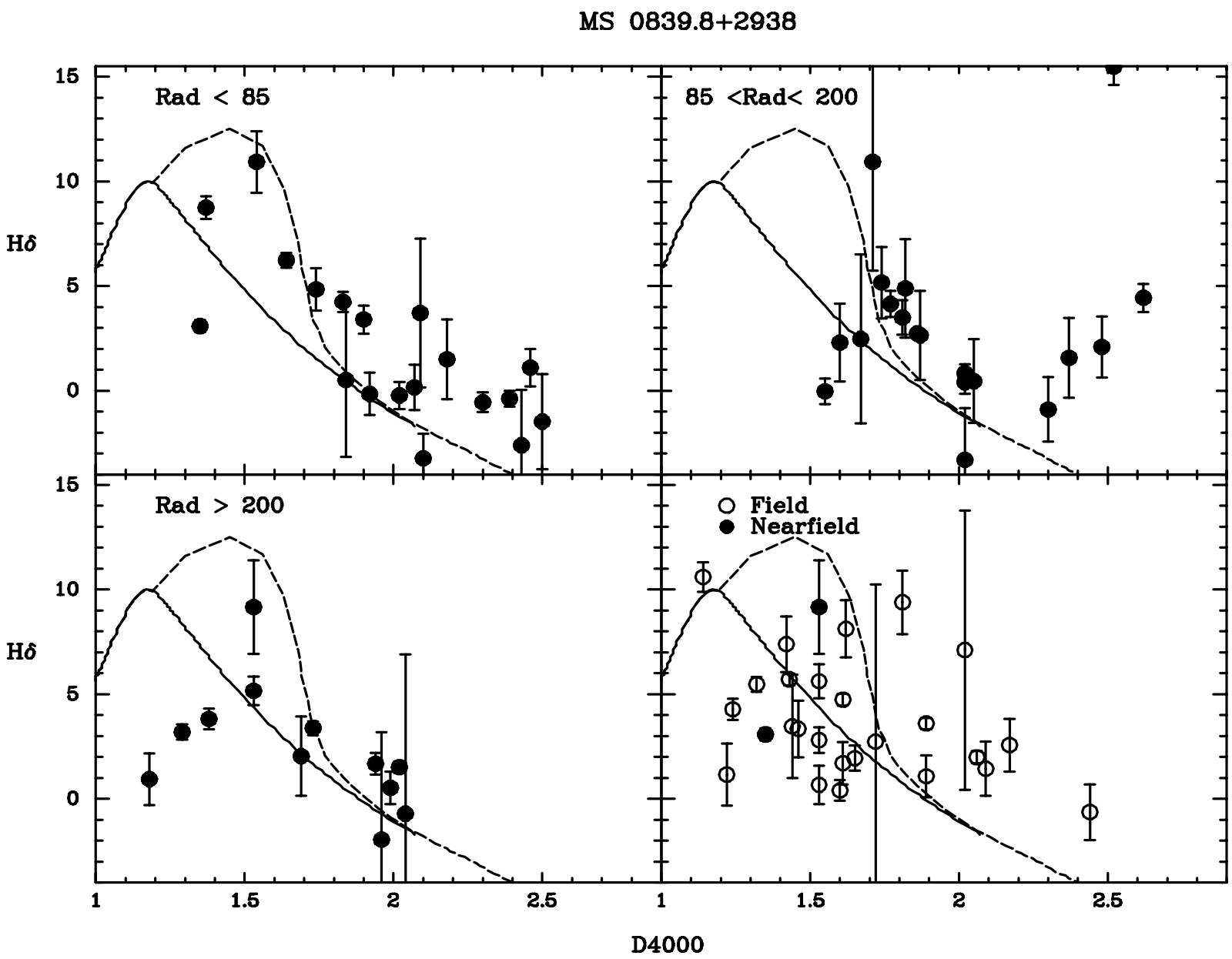
MS 0839.8+2938
Rad < 85
85 <Rad< 200
Rad > 200
Field
Nearfield
Hδ
Hδ
D4000
15
10
5
0
1
1.5
2
2.5

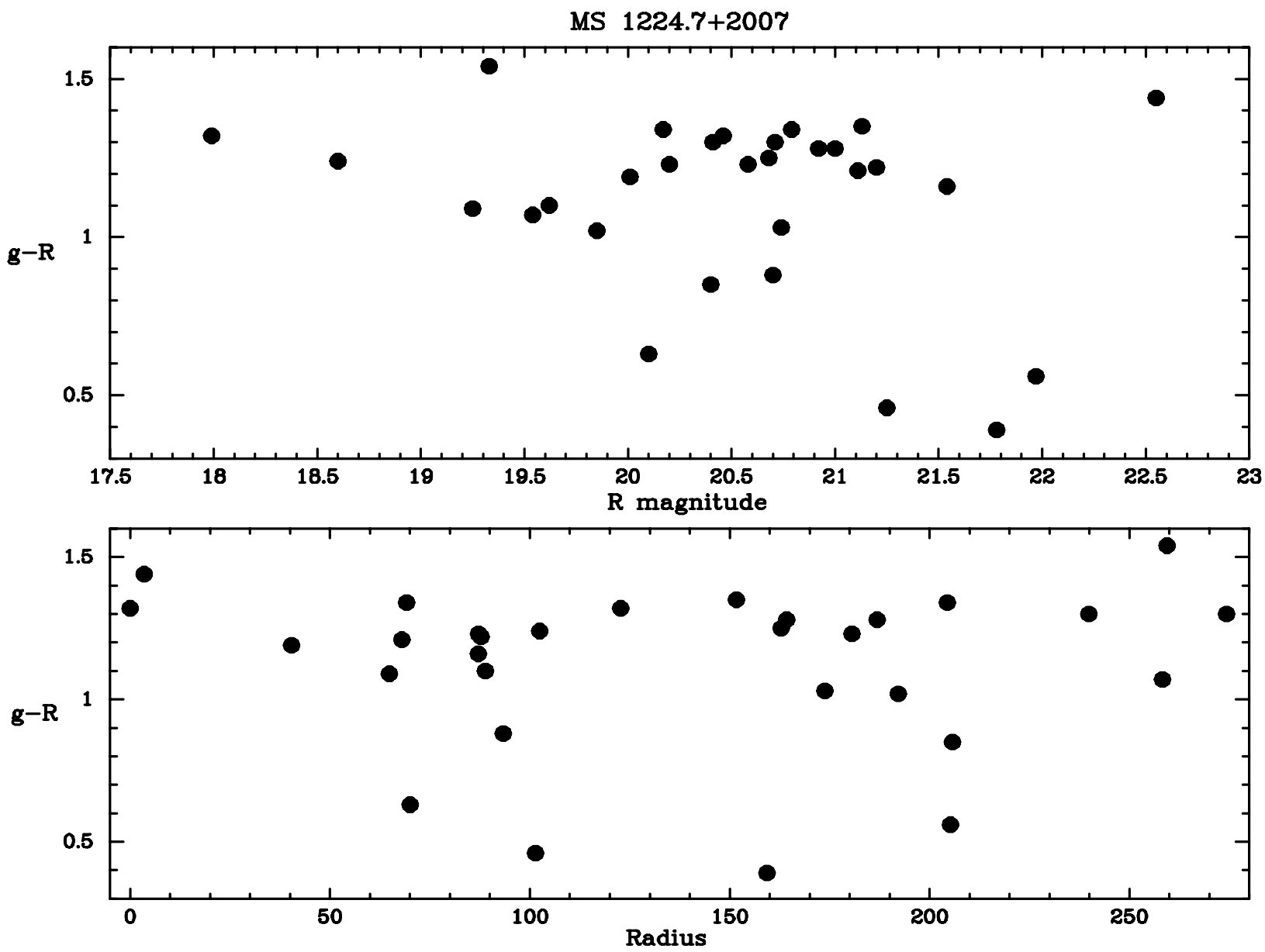
MS 1224.7+2007
g−R
1.5
1
0.5
17.5
18
18.5
19
19.5
20
20.5
21
21.5
22
22.5
23
R magnitude
g−R
1.5
1
0.5
0
50
100
150
200
250
Radius

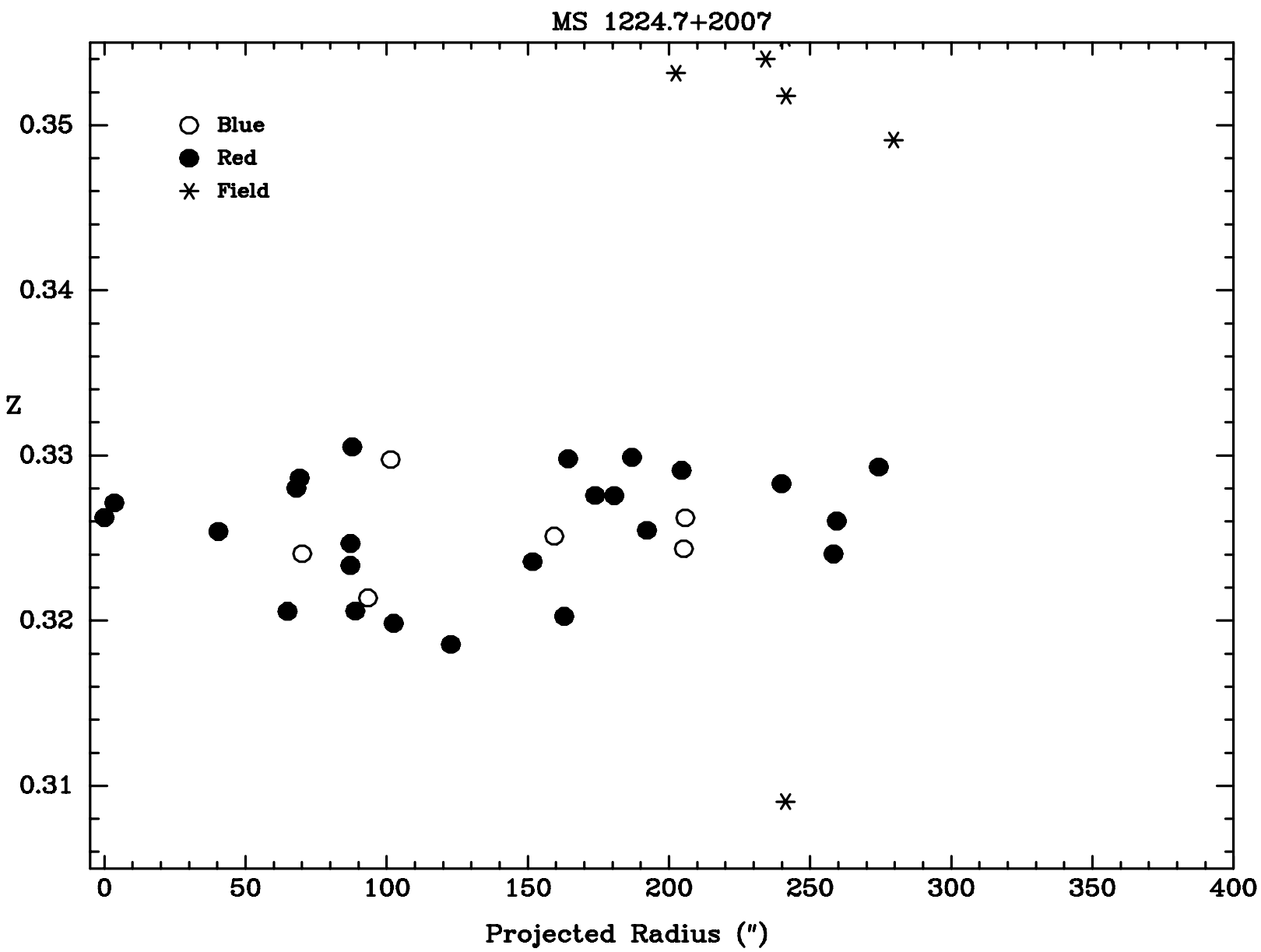
MS 1224.7+2007
Blue
Red
Field
0.35
0.34
0.33
0.32
0.31
z
0
50
100
150
200
250
300
350
400
Projected Radius (")

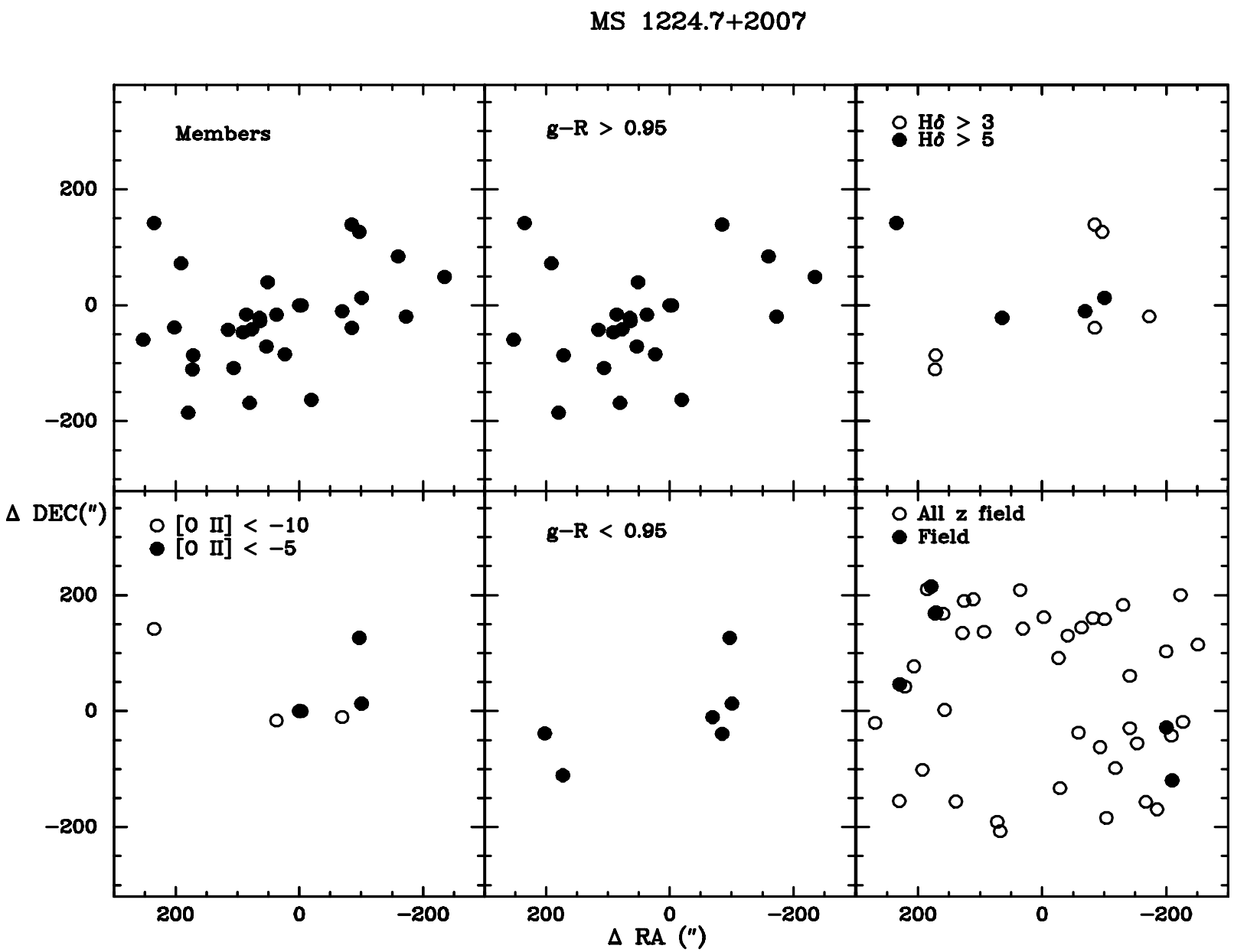
MS 1224.7+2007
Members
g−R > 0.95
Hδ > 3
Hδ > 5
[O II] < −10
[O II] < −5
g−R < 0.95
All z field
Field
Δ DEC(″)
Δ RA (″)
200
0
−200

This figure "fig10.gif" is available in "gif" format from:

http://arXiv.org/ps/astro-ph/9912148v1

This figure "fig11.gif" is available in "gif" format from:

http://arXiv.org/ps/astro-ph/9912148v1

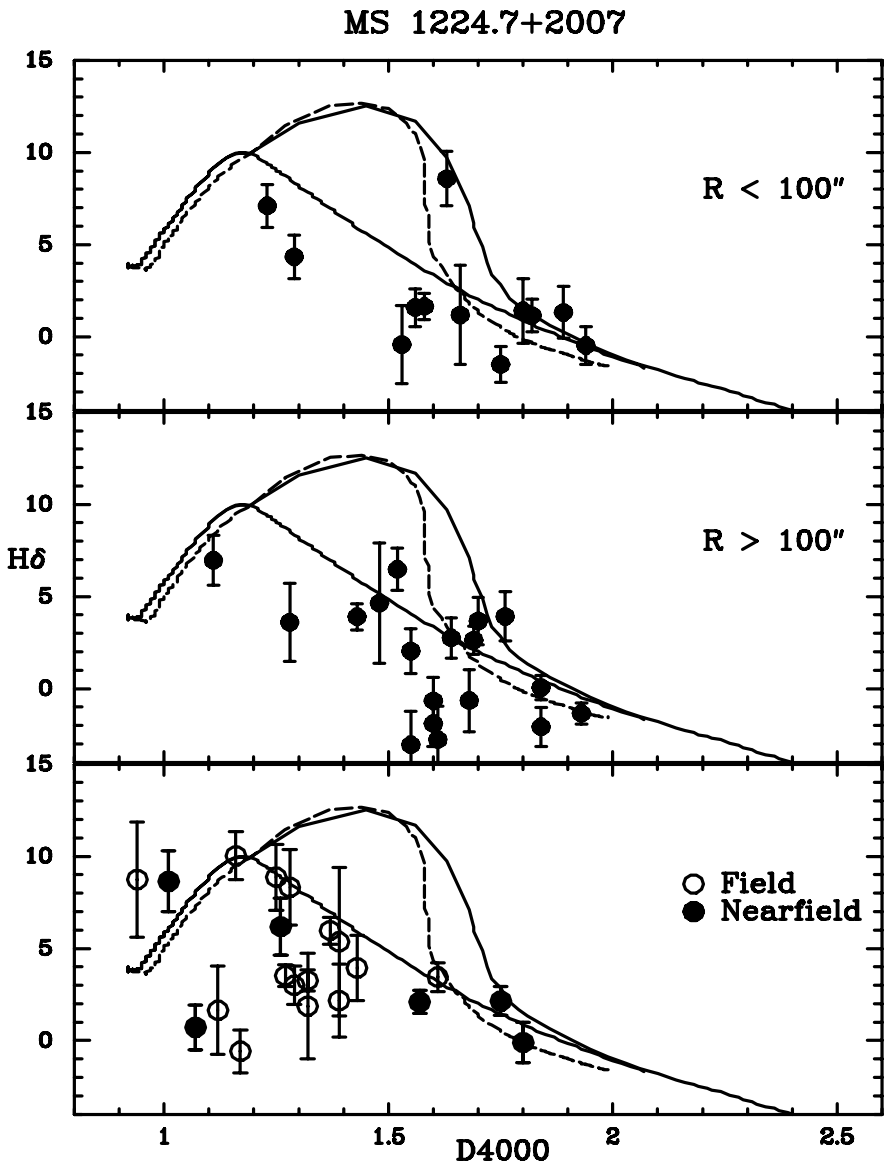
MS 1224.7+2007
R < 100″
R > 100″
Hδ
Field
Nearfield
D4000
15
10
5
0
1
1.5
2
2.5

This figure "fig13.gif" is available in "gif" format from:

http://arXiv.org/ps/astro-ph/9912148v1

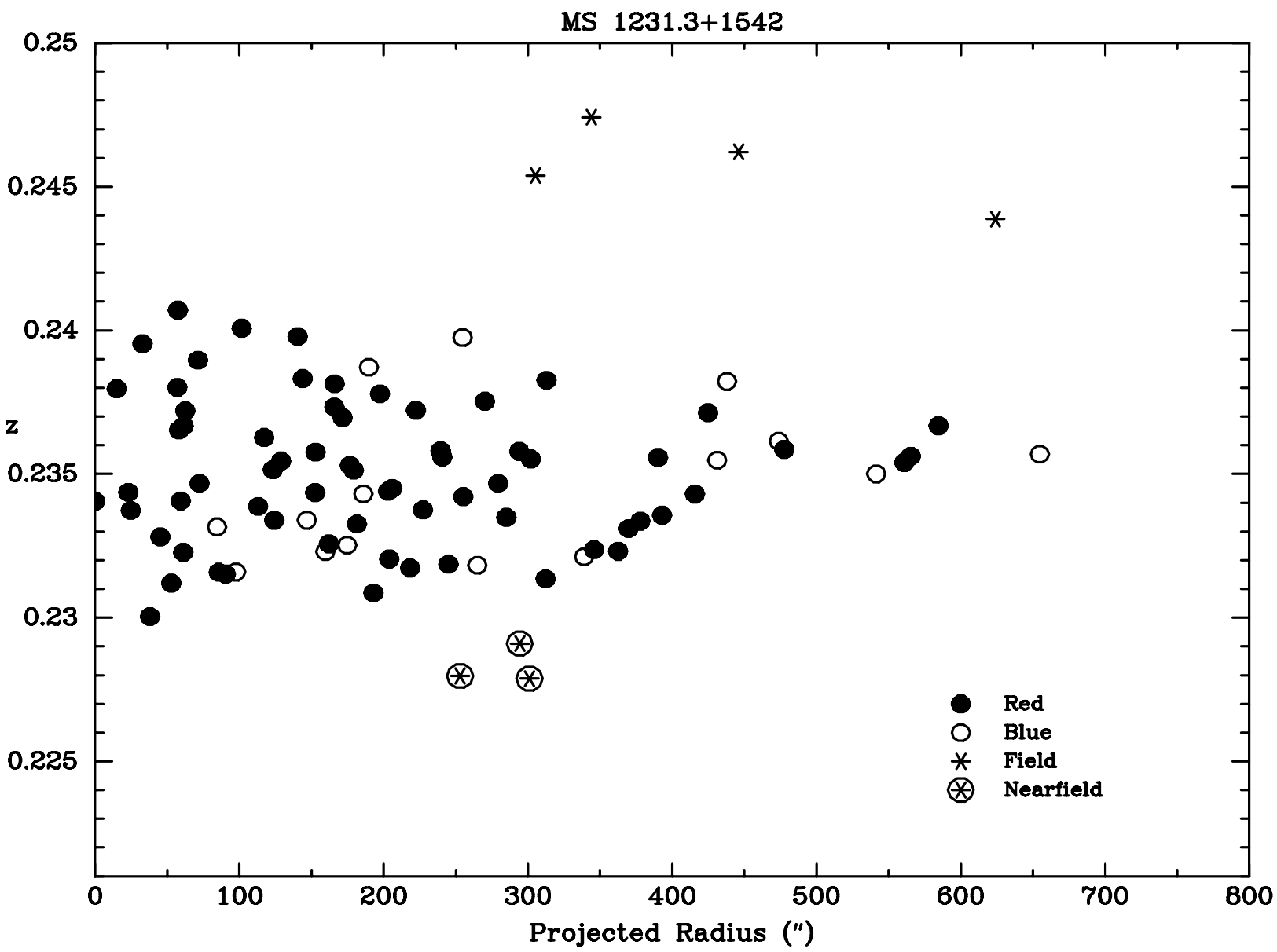
MS 1231.3+1542
0.25
0.245
0.24
0.235
0.23
0.225
z
0
100
200
300
400
500
600
700
800
Projected Radius (")
Red
Blue
Field
Nearfield

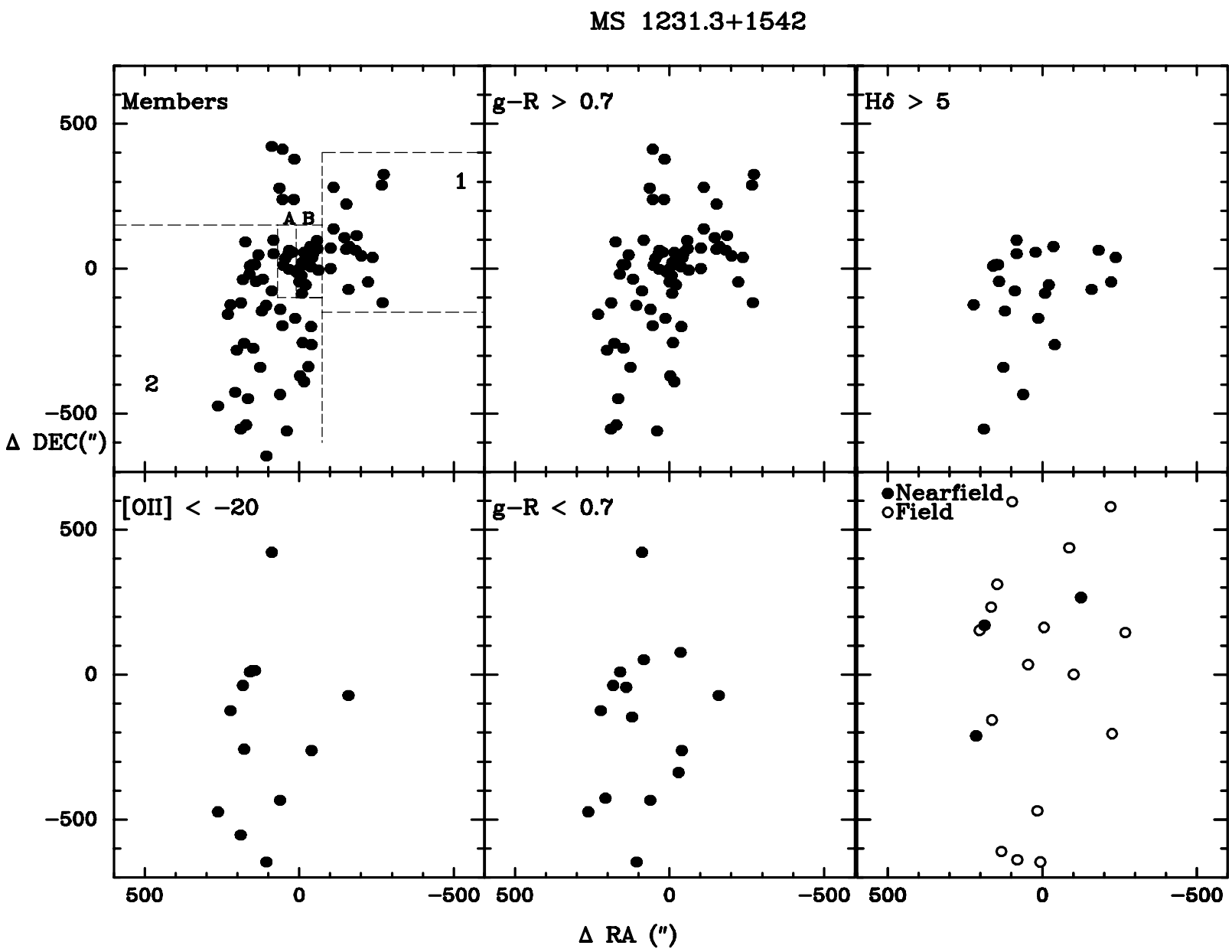
MS 1231.3+1542
Members
g−R > 0.7
Hδ > 5
[OII] < −20
g−R < 0.7
Nearfield
Field
1
2
A
B
500
0
−500
Δ DEC(")
Δ RA (")

This figure "fig16.gif" is available in "gif" format from:

http://arXiv.org/ps/astro-ph/9912148v1

This figure "fig17.gif" is available in "gif" format from:

http://arXiv.org/ps/astro-ph/9912148v1

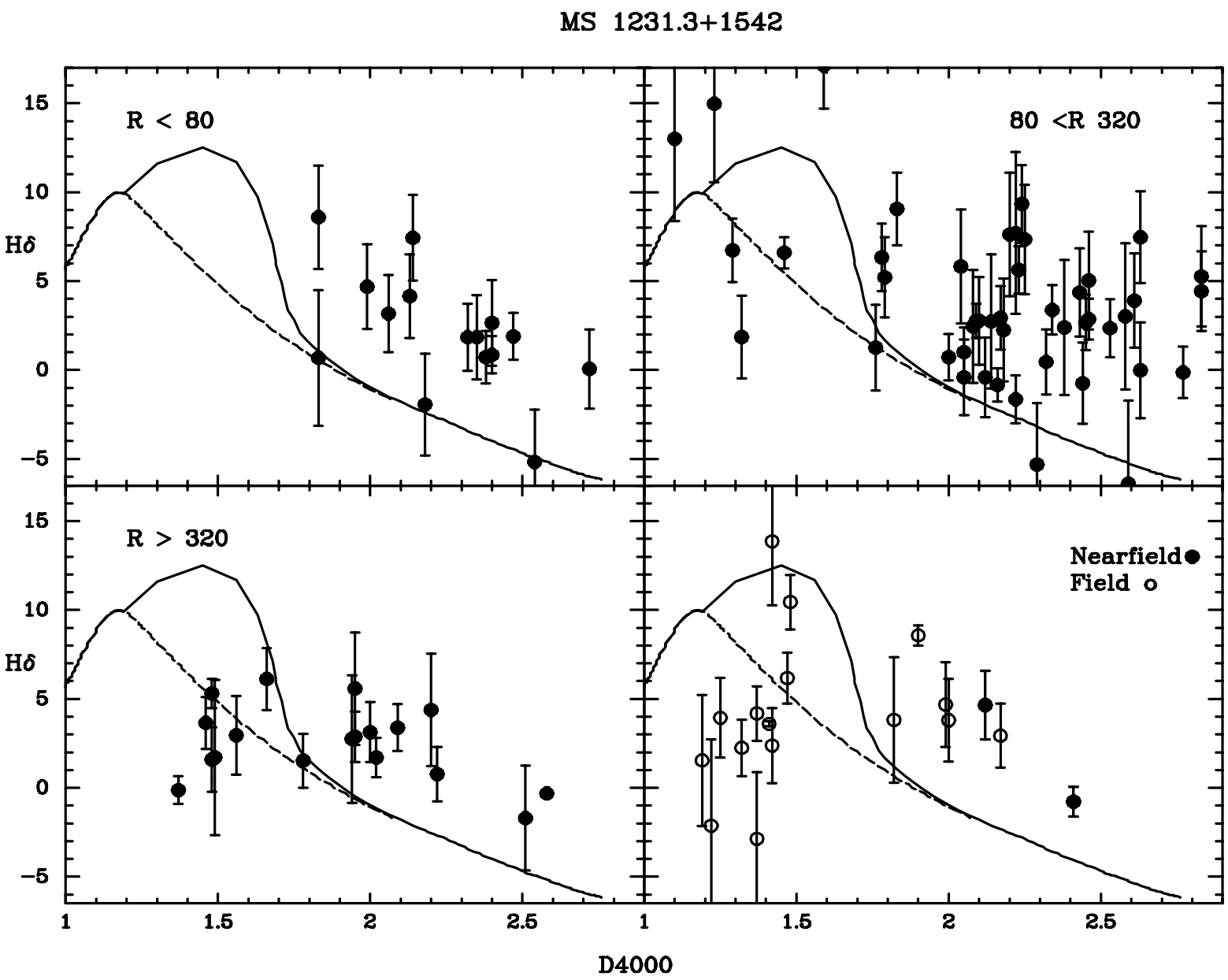
MS 1231.3+1542
R < 80
80 <R 320
R > 320
Nearfield●
Field o
Φ
Hδ
Hδ
D4000
15
10
5
0
−5
1
1.5
2
2.5

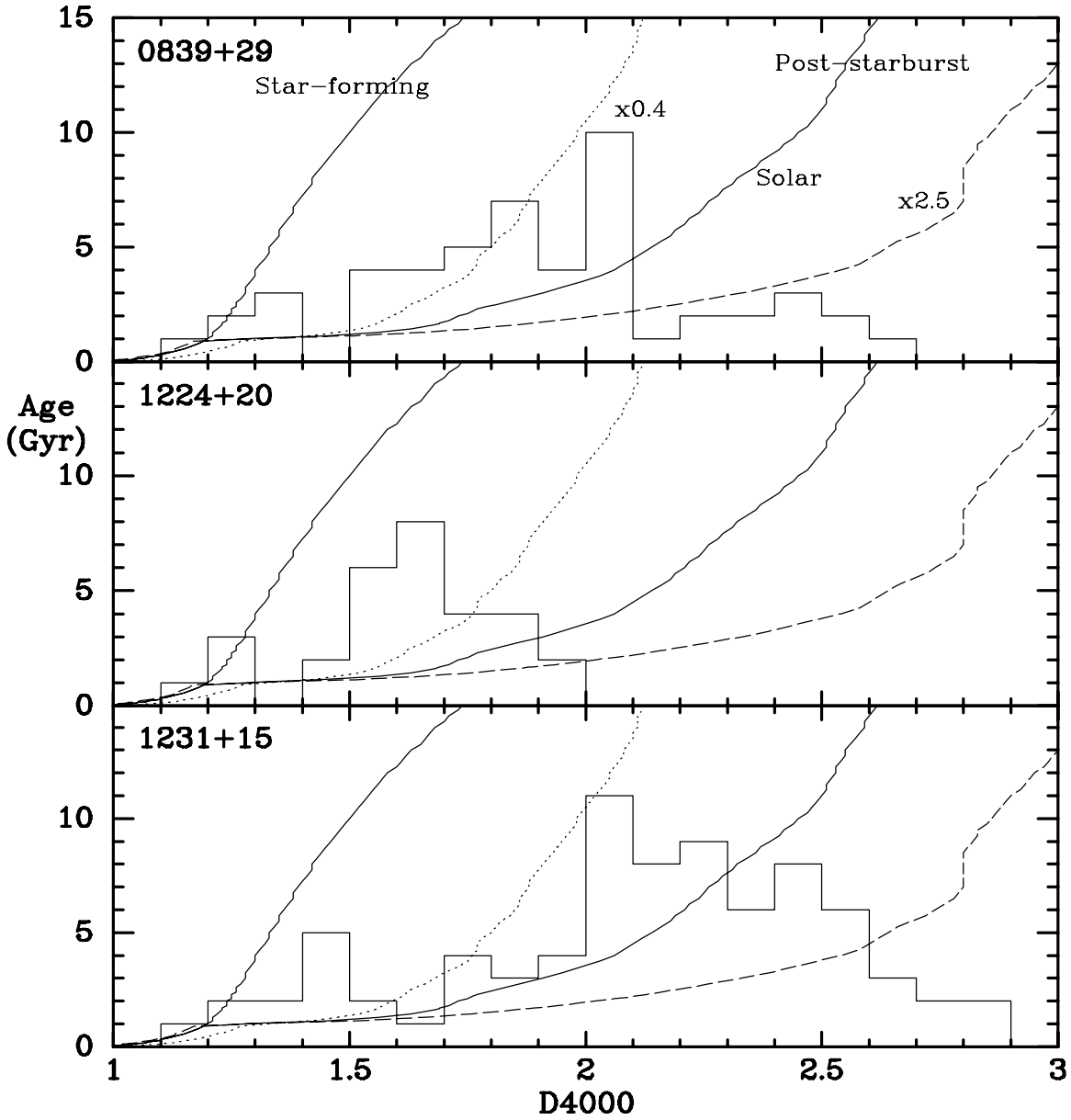
0839+29
Star−forming
x0.4
Post−starburst
Solar
x2.5
1224+20
1231+15
Age
(Gyr)
D4000
0
5
10
15
1
1.5
2
2.5
3

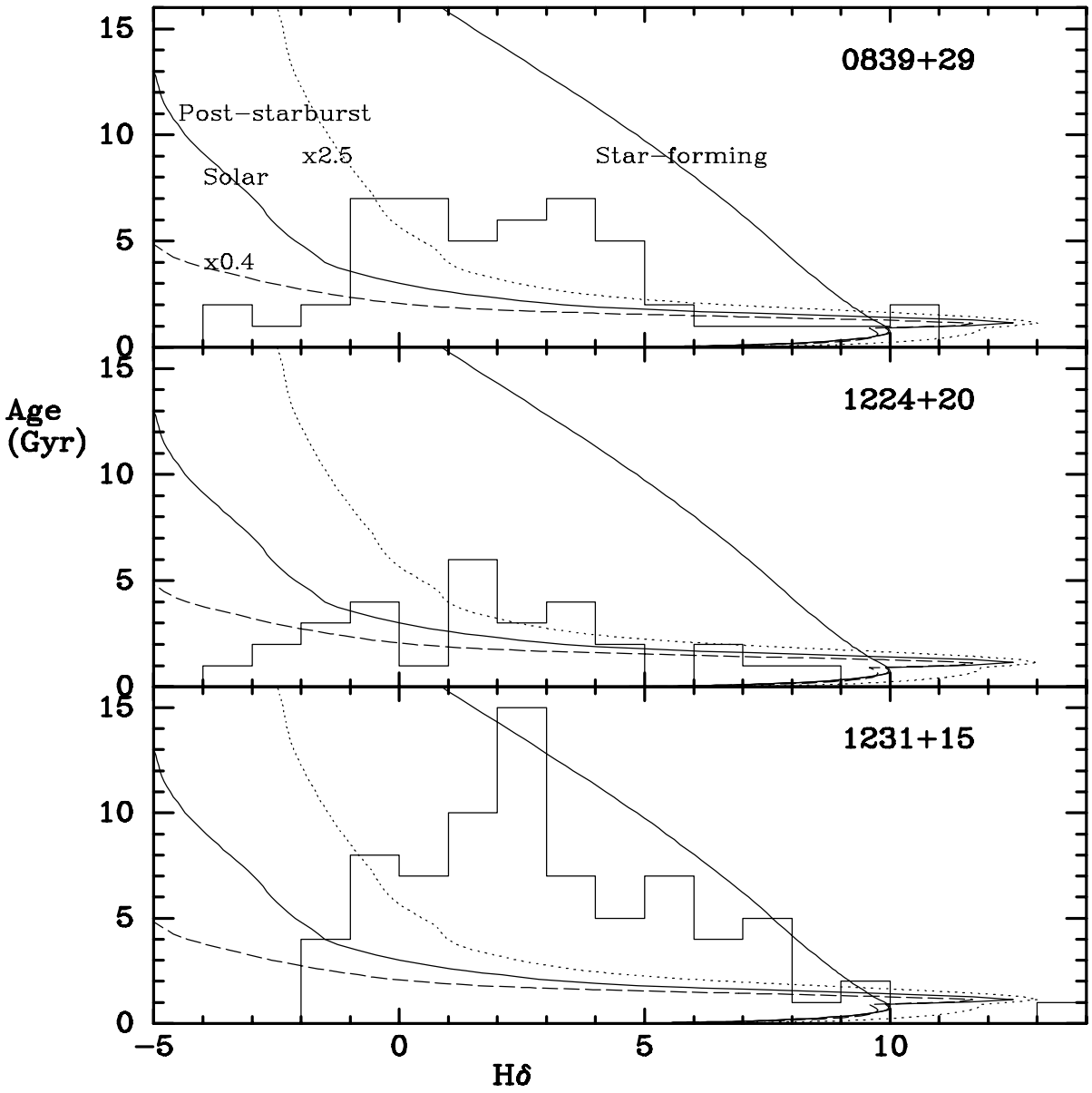
0839+29
1224+20
1231+15
Post−starburst
x2.5
Solar
x0.4
Star−forming
Age
(Gyr)
Hδ
15
10
5
0
−5
0
5
10